FRACTURE TOUGHNESS OF SMALL SPECIMENS CONTAINING SURFACE CRACKS

D.L.Chen*, B.Weiss* and R. Stickler*

Modified surface-crack tension specimens according to ASTM E 740 were tested by the standard plane-strain fracture test procedure to determine the fracture toughness of various materials at room temperature. It was found that the surface-crack tension test procedure can generally yield a valid fracture toughness value if the tested material exhibits negligible stable subcritical crack growth prior to the tensile fracturing. For the materials in which significant stable subcritical crack propagation occurs prior to failure, it seems necessary to determine alternatively an initiation stress intensity value of the subcritical crack growth. The applicability, advantages and limitations of the test procedure are discussed.

INTRODUCTION

Since Griffith´s fundamental considerations it has been recognized that the fracture strength of materials is not a characteristic material property, but a parameter that is closely related to the sizes of defects, flaws and cracks existing in the materials (Sakai and Bradt (1)). The presence of a crack reduces the fracture strength of an engineering component and this strength decreases progressively with increasing crack size. Conventional tensile tests cannot accurately predict the fracture resistance of a material, a more appropriate criterion for characterizing such a resistance is the fracture toughness as determined by standard test procedures.

The standard plane-strain fracture toughness tests following ASTM E 399 (2) requires a minimum specimen size to ensure plane-strain conditions to prevail along a major portion of the crack front during the test. This criterion makes testing of many materials and product forms impractical. In addition, this ASTM test procedure requires fatigue precracking to achieve a sharp crack which for many high-strength low-ductility materials is difficult to realize because of unexpected failure during the precracking.

Several modified test methods have been proposed in the literature which permit the use of smaller specimens (Wang and Pilliar (3)). These methods require special evaluation procedures but may not always yield true plane-strain fracture toughness values. It has been stated that although valid K_{IC} values are certainly very useful one should keep in mind that the application of a toughness value should be

* Institute for Physical Chemistry - Materials Science, University of Vienna
Währinger Straße 42, A - 1090 Vienna, Austria

relevant to the particular geometry and thickness (Broek (4)). One need not strictly adhere to a valid K_{IC} value irrelevant to the practical application.

In practice, technical structures are known to contain often part-through semi-elliptical surface cracks. Thus, the fracture toughness data determined directly from surface-crack specimens seem to have a more practical significance. A test procedure using this type of specimens was also recommended in ASTM E 740 (5) in which the tested metallic materials should not be restricted by strength, thickness or toughness. The present investigation is aimed to examine the applicable range of the proposed test procedure by selecting different materials and to indicate further some appropriate experimental modifications.

MATERIALS AND EXPERIMENTAL PROCEDURES

Several kinds of PM materials involving molybdenum and a Mo alloy, an aluminium alloy manufactured from rapid solidified powder and sintered steel with different porosities were chosen for this investigation. The chemical composition is listed in Table 1.

TABLE 1- The Composition and Microstructures of the selected Specimen Materials.

PM Mo (in ppm): 13 O_2, 10 C. as-swaged rod, recrystallized rod and forged bar (fine grain).
PM Mo-Ti-Zr alloy (in ppm): 4700 Ti, 820 Zr, 305 C, 170 O_2. recrystallized rod and forged bar.
PM Al-Fe-Mo-Zr alloy (in wt%): 8 Fe, 2 Mo, 1 Zr. fine grained recrystallized.
PM Fe-Mo steel (in wt%): 1.5 Mo, 0.7 C. sintered with different porosities.

Mo and the Mo alloy were tested in rod-shaped product form in either the as-swaged or in a recrystallized condition. The PM Fe-Mo steel was manufactured to contain porosities of 6.6% and 11.4%, respectively. The Al-Fe-Mo-Zr alloy was fabricated from powders produced by the rapid solidification technique. The tensile properties of these materials are shown in Table 2.

TABLE 2- Tensile Properties of the Test Materials.

Material	R_m [MPa]	R_{eL} [MPa]	R_{eH} [MPa]	$R_{p0.2}$ [MPa]	A [%]	HVI0
Mo, as-swaged (rod)	659	655	749	-	40	234
Mo, recrystallized (rod)	400	-	-	361	50	183
Mo, forged bar	480	-	-	420	10	247
Mo-Ti-Zr, recrystallized (rod)	581	443	536	-	30	210
Mo-Ti-Zr, forged bar	720	-	-	700	2	270
Al-Fe-Mo-Zr alloy	530	-	-	455	10	-
Fe-Mo steel, 6.6% porosity	1370	-	-	-	-	-
Fe-Mo steel, 11.4% porosity	1170	-	-	-	-	-

Dumbbell-shaped specimens with a rectangular gauge section were machined from the rod-shaped materials (see Fig.1, as an example). In these specimens the crack plane was oriented in the radial direction normal to the forging direction. In order to compare the fracture toughness data obtained from the surface-crack tension specimens with those measured from the conventional through-thickness plane-strain specimens, some disk-shaped compact tension (DCT) specimens (according to Fig. A6.1 in ASTM E 399-83) of hot-forged and subsequently air-cooled bars of Mo and Mo-Ti-Zr alloy were selected, as shown in Fig.2. The specimens were machined out of circular sections cut normal to the axis of the bars with deformed microstructure of grains elongated in the forging direction, i.e., the crack plane was oriented in the radial direction parallel to the forging direction.

The test procedure based on ASTM E 740 recommendations with an appropriate modification was utilized to determine the fracture toughness of various materials. The central portion of the gauge section, as shown in Fig.1, was metallographically polished, and subsequently a lancet-shaped surface starter notch (2 mm long, 1 mm deep) at the center of the test section was introduced by electrical discharge machining to initiate the required fatigue crack. Fatigue crack initiation and propagation tests were performed with a resonance testing system operated at 20 kHz under axial loading, R=-1 and room temperature (Weiss and Stickler (6)). To obtain a fatigue crack with a tip as sharp as possible and the plastic zone at the crack tip as small as possible, a load-shedding procedure during precracking was used to determine the fatigue threshold. The surface crack length was monitored by a traveling light microscope coupled with a video system with a resolution of about 10 μm.

Values of the fracture toughness for such surface-crack specimens were calculated in terms of the equation derived by Newman and Raju (7). This relationship can be used over a wider range of crack length, i.e., $a<c$, $a<t$, $2c<0.5W$ (a is the crack depth, 2c the surface crack length, t is the specimen thickness, W is the specimen width). Thus, in the present investigation the length (2c) of the fatigue precrack, i.e., the crack length corresponding to the fatigue threshold, is not restricted by the requirement of $W>10c$ in ASTM E740 (5). For the specimen shown in Fig.1 the precrack was of the length of approximately 0.5 W, i.e., $2c = 5\sim6$ mm. The shape of the fatigue precrack required for the calculation of fracture toughness values were determined from an evaluation of the fracture surfaces exposed by the following tensile testing.

Different loading rates below the recommended maximum value of 690 MPa/min were applied in a tensile testing machine for the subsequent fracturing tests of the precracked specimens. For most tensile tests the crack opening displacement (COD) was measured with a strain gauge applied across the center of the crack. The curves of load-COD were recorded during the tests.

For low-toughness materials for which stable subcritical crack growth prior to failure is generally absent, the fracture mechanics characterization based on the original crack dimensions and the maximum load, i.e., so-called residual strength, on the load-COD curve is appropriate. For tough materials such a characterization was pointed out to be questionable if significant stable crack growth occurs prior to failure.

If the stable subcritical growth of surface cracks occurs under rising load, the recorded load-COD behavior is not linear. As schematically shown in Fig.3, an evaluation procedure suggested by Chen (8) resulted in three fracture toughness values corresponding to P_i, P_Q and P_e (or P_{max}) applicable for PM-materials.

Attempts to initiate fatigue cracks under cyclic loading at a stress ratio of R = 0.1 resulted in a spontaneous failure of the DCT specimen without an indication of the formation of a fatigue crack (9). Precracking experiments of this type of specimens were carried out under compressive cycling (R = 0.1 in compression). After fatigue precracking the specimens were fractured in tension at the recommended loading rate and the load/crack opening displacement (P-COD) curves were recorded (the COD signal was obtained from a strain gauge applied across the notch near the fatigue precrack).

The evaluation of the recorded P-COD curves requires the determination of P_Q (load at intersection with 95% elastic slope secant, see also Fig.3) according to ASTM E399 (2). If the ratio of P_{max}/P_Q is smaller than 1.1, implying that the initial instability is close enough to the final catastrophic instability, or if the quantity of $B_{min}(=2.5(K_Q/s_{ys})^2)$ is less than both the actual specimen thickness (B_{act}) and the crack length, the calculated K_Q can be considered to be a valid K_{IC} value of the material being tested. The stress intensity factor for DCT specimen was calculated according to the following equation,

$$K_I = \frac{P}{t\sqrt{W}} f_1$$

$$f_1 = \frac{(2+a/W)\left[0.76+4.80(a/W)-11.58(a/W)^2+11.43(a/W)^3-4.08(a/W)^4\right]}{\sqrt{(1-a/W)^3}}$$

with P the applied load and W the equivalent specimen width (Murakami, et al., (10)).

EXPERIMENTAL RESULTS AND DISCUSSION

An example of the near-threshold fatigue crack propagation behavior obtained during precracking is shown in Fig.4. It can be seen that the obtained value for the fatigue threshold of the PM Al-Fe-Mo-Zr alloy is 2.0 MPa$\sqrt{m}$. Fig.5 gives several typical crack shapes of (a) as-swaged Mo, (b) recrystallized Mo-Ti-Zr alloy and (c) Al-Fe-Mo-Zr alloy. One can see from these fractographs that the recrystallized Mo-Ti-Zr material exhibits a fair amount of stable subcritical crack growth, whereas in the as-swaged Mo and the Al-Fe-Mo-Zr alloy almost no stable crack propagation occurs.

The fracture toughness values determined from the surface-crack tension specimens with an accuracy of ±10% are listed in Table 3. It should be noted that most of the data listed in Table 3 are averaged from 2-8 duplicate tests, except those given within brackets. From this table it can be seen that irrespective of as-swaged or recrystallized Mo, no stable subcritical crack growth was observed (also Fig.5(a)), resulting in the same K_{Ii}, K_{IQ} and K_{Ie} values for each state and equivalent fracture toughness values for both material states. Therefore, the obtained values are considered as valid fracture toughness K_{IC}. However, the forged bar Mo exhibited considerable subcritical crack growth, giving rise to a higher K_{Ie} value. The

evaluated K_{Ii} value, representing the initiation of subcritical crack propagation during the tensile loading, is equivalent to that obtained for as-swaged or recrystallized Mo.

TABLE 3- Fracture Toughness Values obtained from Surface-crack Tension Specimens (Fig.1) machined of various Specimen Materials, Accuracy ±10%.

Material	K_{Ii} [MPam$^{1/2}$]	K_{IQ} [MPam$^{1/2}$]	K_{Ie} [MPam$^{1/2}$]	SSCG#	B_{min}* [mm]	B_{act} [mm]
Mo, as-swaged (rod)	17	17	17	no	1.7	4
Mo, recrystallized (rod)	18	18	18	no	6.2	5
Mo, forged bar	17	21	40	yes	6.3	5
Mo-Ti-Zr, recrystallized (rod)	(13)	(19)	31	yes	4.6	5
Mo-Ti-Zr, forged bar	17	17	17	no	1.5	5
PM Al-Fe-Mo-Zr alloy	8	8	8	no	0.8	5
Fe-Mo steel, 6.6% porosity	25	33	36	no	1.5	6
Fe-Mo steel, 11.4% porosity	(14)	(20)	(23)	no	0.7	6

#SSCG --- Stable subcritical crack growth;
*The minimum specimen thickness required according to ASTM E 399.

TABLE 4- Fracture Toughness Values obtained from standard Disk-shaped CT Specimens (Fig.2) machined from various Specimen Materials. Comparison with Literature Data (CT Specimen), Accuracy ±10%.

Material	K_{IC} [MPam$^{1/2}$]	Specimen type	Stable crack growth
Mo, forged bar	8	DCT	no
Mo-Ti-Zr, forged bar	19	DCT	no
Al-Fe-Mo-Zr alloy	7.3*	CT	no

* Data taken from Ref. 11

The experimental observations show that the forged bar of Mo-Ti-Zr alloy exhibited no subcritical crack propagation, while almost all the recrystallized Mo-Ti-Zr specimens indicated stable crack growth (Fig.5(b)) and hence led to a larger K_{Ie} value. Moreover, no or negligible stable subcritical crack propagation could be observed for the PM Al-Fe-Mo-Zr alloy (Fig.5(c)) and for the PM Fe-Mo steel.

Fracture toughness values obtained from standard DCT specimens are summarized in Table 4. By comparing the data listed in Table 3 and Table 4 one can notice that for the forged bar of Mo the K_{IC} value obtained from DCT specimen is smaller than that measured from the surface-crack specimen. This may be due to the difference in the crack plane orientation relative to the deformation axis, which may result in an stable subcritical crack growth during the tensile loading. The fracture

toughness data for the various Mo specimens reflect the different material conditions (heat treatment, resulting microstructure and its anisotropy) and crack orientation (9).

If no subcritical crack propagation occurs prior to the tensile fracturing for both surface-crack tension and DCT (or CT) specimens, the fracture toughness values obtained from the two types of specimens are comparable, as demonstrated in Table 3 and Table 4 for forged bar Mo-Ti-Zr and Al-Fe-Mo-Zr alloys. In this case the influence of the orientation of the crack plane relative to the rolling direction for the forged bar Mo-Ti-Zr alloy appears negligible. From these experimental results it can be concluded that both test methods can generally yield equivalent fracture toughness data for homogenous and low-toughness materials. If the tested material do exhibit the stable subcritical crack growth, not only K_{Ie} data as suggested in ASTM E740, but also the K_{Ii} or K_{IQ} value in the surface-crack tension test should be evaluated.

Preliminary tests with the surface-crack tension specimens of recrystallized Mo-Ti-Zr alloy indicated only a little effect of the precrack depth on K_{Ie} value for the selected region in the present investigation, as shown in Fig.6. The obtained K_{Ie} values as a function of the loading rate for the recrystallized Mo-Ti-Zr material is illustrated in Fig.7. It can be seen that over a wide range of the loading rates between 20 and 650 MPa/min only a negligible influence of loading rate was observed. This experimental result coincides with the statement given in ASTM E740. Further investigations are needed to reveal the influence of test temperature on the fracture toughness in view of the temperature sensitivity of the strength of these materials.

The surface-crack tension test procedure offers the advantages of less specimen material needed, simple specimen preparation, short experimental times for fatigue precracking at low amplitudes even of brittle materials and its applicability to test small rod-shaped specimen. Testing of sheet metallic materials may appear feasible.

CONCLUSIONS

From a comparison of the fracture toughness data of various materials, obtained from standard CT (or DCT) specimens and from surface-crack tension specimens, the following conclusions can be drawn:

1. For low-toughness materials exhibiting no or negligible stable subcritical crack growth prior to the tensile fracturing, the obtained K_{Ie} value from surface-crack tension tests, based upon the maximum load and the shape and sizes of fatigue precrack, can generally reflect the fracture toughness determined from standard CT specimens. The extent of fulfillment of the ASTM size requirement can be deduced from the values of B_{min} and B_{act} listed in Table 3. It can be seen that the thickness of the Mo-materials with the lower yield strength is insufficient.

2. For the test materials exhibiting significant stable subcritical crack propagation prior to failure, the application of K_{Ie} data may result in a non-conservative estimate of the resistance of the material to fracture. In these cases the use of K_{Ii} or K_{IQ} appears more appropriate.

3. The surface crack tension test procedures applied in this investigation should be of value for a fracture toughness characterization, with little testing efforts, of brittle metals and alloys in their practical product forms such as forged bars, swaged rods, or plate products.

ACKNOWLEDGEMENTS

The authors thank Mr.H.Hödl, Mr.D.Spoljaric, Dr.H.Schmidt and Dr.W.Pichl for their assistance in the experimental work. The Mo-based specimen material was supplied by the Metallwerk Plansee GmbH, Reutte.

REFERENCES

(1) Sakai, M. and Bradt, R.C., Inter. Mater. Rev., Vol. 38, No. 2, 1993, pp. 53-78.

(2) ASTM E 399-83, "Standard Test Method for Plane-Strain Fracture Toughness of Metallic Materials".

(3) Wang, C.T. and Pilliar, R.M., J. Mater. Sci., Vol. 24, 1989, pp. 2391-2400.

(4) Broek, D., "Elementary Engineering Fracture Mechanics", M.Nijhoff Publ., Boston, 1982.

(5) ASTM E 740-88, "Standard Practice for Fracture Testing with Surface-Crack Tension Specimens".

(6) Weiss, B. and Stickler, R., "Ultrasonic Fatigue", edited by J.M.Wells, et al, The Metallurgical Society of AIME, 1982, pp.135-171.

(7) Newman, J.C., Jr. and Raju, I.S., Eng. Fract. Mech., Vol.15, 1981, pp. 185-192.

(8) Chen, Y.T., "Properties, Evaluation and Testing of P/M Materials", Metal Powder Industries Federation, Princeton, New Jersey, 1988, pp. 99-124.

(9) Chen, D.L., Weiss, B., Stickler, R., Witwer, M., Leichtfried, G. and Hödl, H., "Metallic High Temperature Materials", Proceedings of the 13th International Plansee Seminar, edited by H.Bildstein and R.Eck, Plansee Metall AG., Reutte, Austria, 1993, pp. 621-631.

(10) Murakami, Y., et al, "Stress Intensity Factors Handbook", Pergamon Press, Oxford, 1987, Vol.1, p.21.

(11) Schäfer, R., "Mechanical Properties and Microstructure of High-Temperature PM Aluminium Alloys", COST 503 Report TF-2976, Industrieanlagen-Betriebsgesellschaft mbH, 1992.

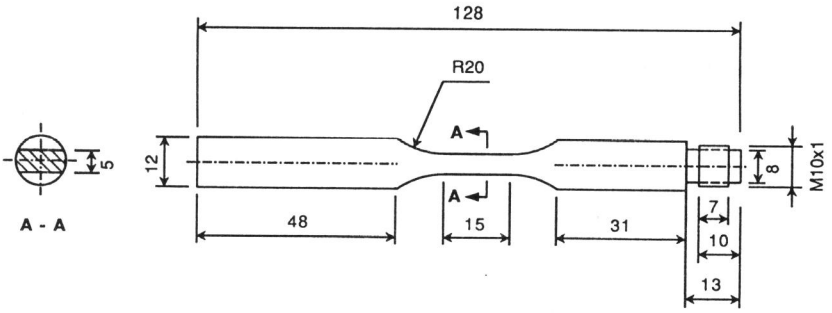

Figure 1 Typical geometry and dimensions of surface-crack tension specimen.

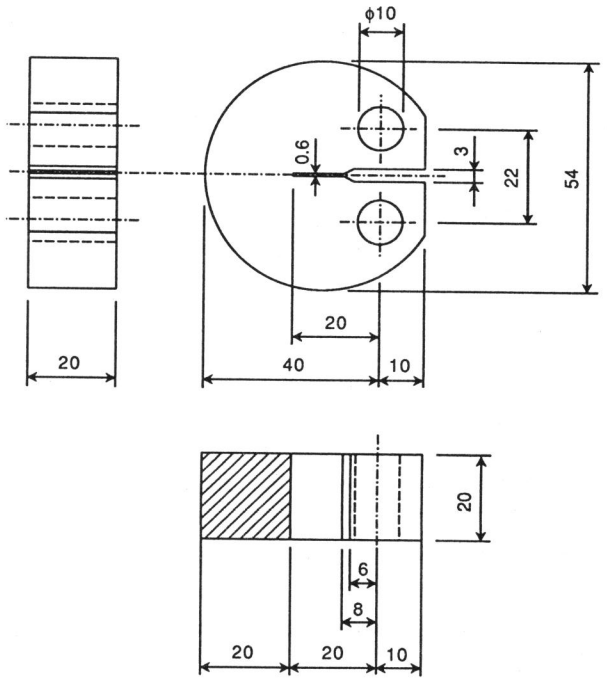

Figure 2 Typical geometry and dimensions of disk-shaped compact tension specimen.

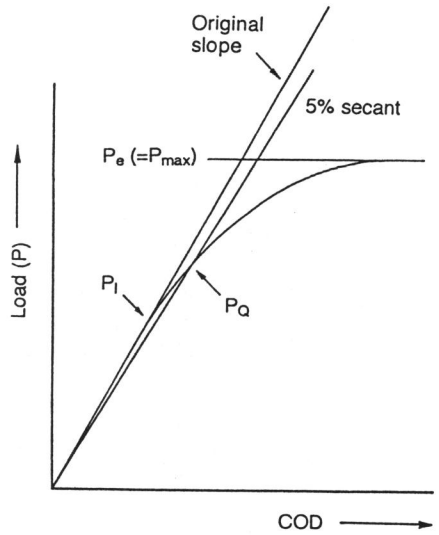

Figure 3 Schematic illustration of load-crack opening displacement curve, defining the various load points.

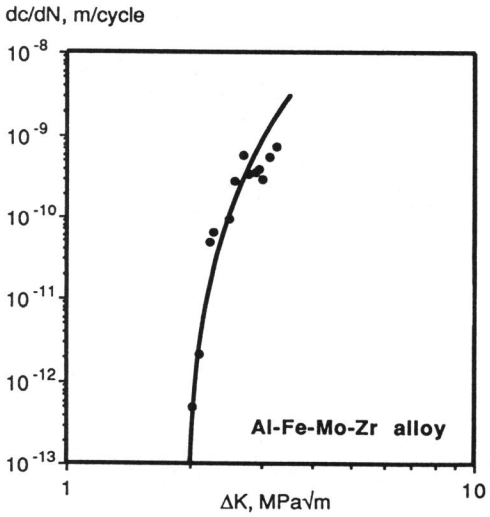

Figure 4 Near-threshold fatigue crack propagation behavior of PM Al-Fe-Mo-Zr alloy, obtained during fatigue precracking under axial loading, 20 kHz, R=-1 and room temperature.

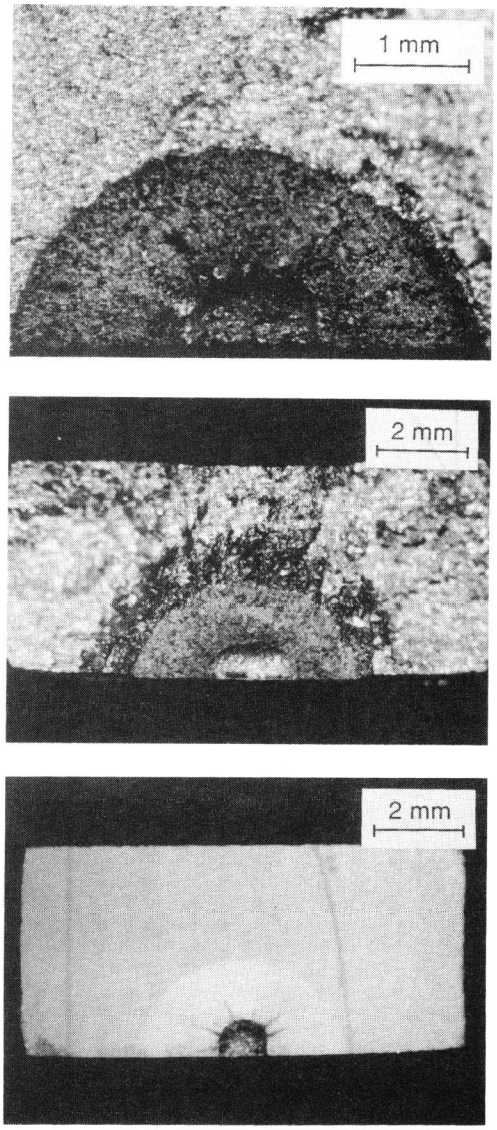

Figure 5 Typical appearances of the fracture surfaces and shapes of fatigue precrack: (a) as-swaged Mo, (b) recrystallized Mo-Ti-Zr alloy, (c) PM Al-Fe-Mo-Zr alloy.

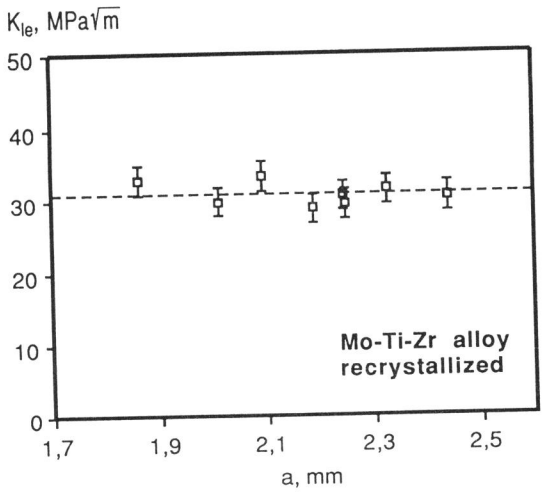

Figure 6 Effect of the crack depth on K_{Ie} values for surface-crack tension specimens of recrystallized Mo-Ti-Zr alloy.

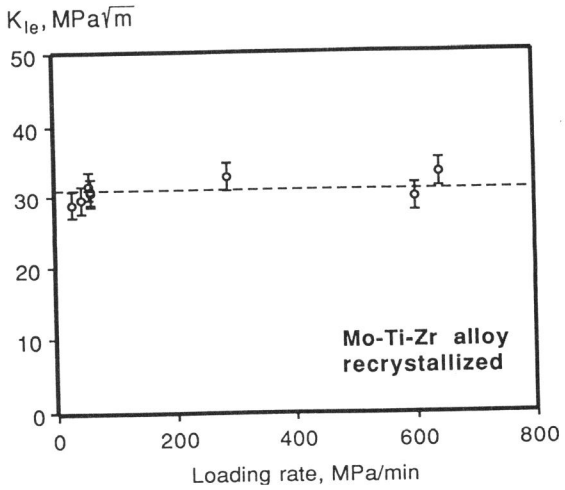

Figure 7 Effect of the loading rate on K_{Ie} values for surface-crack tension specimens of recrystallized Mo-Ti-Zr alloy.